JMEPEG (2011) 20:757–761
DOI: 10.1007/s11665-011-9837-z

1059-9495/$19.00

Production of Nitinol Wire from Elemental Nickel and Titanium Powders Through Spark Plasma Sintering and Extrusion

J. Butler, P. Tiernan, A.A. Gandhi, K. McNamara, and S.A.M. Tofail

(Submitted May 13, 2010; in revised form December 21, 2010)

This study demonstrates the production of highly dense binary NiTi by spark plasma sintering (SPS) of elemental Ni and Ti powders. The sintered billets were extruded to 0.7 mm wire for tensile testing. Excellent mechanical properties and very dense microstructures were obtained in the wires produced in this way. The material demonstrated 4% recoverable strain, 14% elongation at fracture and 630 MPa ultimate tensile stress. Furthermore, a close control of the level of impurities was also possible. This highlights the efficacy of the SPS route in production-capacity manufacture of NiTi products.

Keywords biomaterials, extrusion, powder metallurgy

1. Introduction

The production of shape memory alloys through powder metallurgy (PM) route is currently considered as a way of producing near-net shape and fine-grain material for application in the aerospace, automotive, and biomedical industry (Ref 1-14). In the reported studies, many problems remain, e.g., the high-oxygen content of the sintered alloys compared to melt-cast alloys (Ref 9). It is usually believed that oxygen combines with nickel and titanium to form $Ti_4Ni_2O_x$ ($0 < x \leq 1$) oxides during processing and these oxides are a major cause of embrittlement in NiTi alloys (Ref 5, 9). Very recently, it was reported that the crystallographic data suggests that oxygen stabilizes the intermetallic compound Ti_2Ni with oxygen in solid solution and that the $Ti_4Ni_2O_x$ ($0 < x \leq 1$) oxide description is inappropriate (Ref 15). If starting from elemental powders, NiTi alloys obtained through a PM route (PM-NiTi henceforth) also contain a large amount of the two main secondary phases, such as the stable intermetallics Ti_2Ni and Ni_3Ti. These phases cannot easily be removed by subsequent homogenization treatments (Ref 2, 9).

To obtain suitable mechanical properties in PM-NiTi, pre-alloyed powders are normally used as the starting material. Most production of PM-NiTi uses pre-alloyed powder that are then consolidated either by hot isostatic pressing (HIP) or metal injection molding (MIM) to form the desired near-net shape (Ref 1, 3-5). Research work using elemental powders as feedstock are inconclusive as these samples did not receive any thermo-mechanical working to fully develop their microstructures and mechanical properties (Ref 2, 9-11, 14, 16, 17). The production of NiTi from elemental powders offers cost savings from an economic point of view since it avoids the delicate production of the pre-alloyed powder. It also offers the freedom to choose the final chemistry and any subsequent doping.

Powder metallurgical techniques such as reactive extrusion synthesis, mechanically activated reactive forging synthesis (MARFOS), self-propagation high-temperature synthesis, liquid-phase sintering, explosive shock wave compression, and mechanical alloying have been reported for the production of PM-NiTi from pure elemental powders (Ref 6, 7, 9, 10). Each method has its own advantages, disadvantages, and need further development.

McNeese et al. (Ref 11) successfully HIP'ed elementary mixtures of Ni and Ti and revealed that the use of elemental powders leads to relatively homogeneous test specimens which contained Ti_2Ni precipitates in the matrix. The study, however, does not report the amount of impurities, and the final sintered material was not produced into a form that is suitable for tensile testing. This makes a direct comparison difficult between the mechanical properties of PM-NiTi and those of conventionally produced NiTi.

For consideration in engineering applications, these properties of PM-NiTi materials must be similar to those of conventional NiTi materials. Apart from the general stress strain behavior, elongation at fracture, mechanical fatigue as well as fatigue of shape memory properties are key parameters characterizing the quality and applicability of PM-NiTi in commercial applications.

The purpose of the research presented in this article is to show the feasibility of manufacturing NiTi through spark plasma sintering (SPS) and hot extrusion by using elemental powders as the starting raw materials. SPS shows great potential as a new process for the fabrication of intermetallic compounds (Ref 12-14, 18). In this technique, a pulsed electric

This article is an invited paper selected from presentations at Shape Memory and Superelastic Technologies 2010, held May 16-20, 2010, in Pacific Grove, California, and has been expanded from the original presentation.

J. Butler, P. Tiernan, A.A. Gandhi, K. McNamara, and **S.A.M. Tofail**, Materials and Surface Science Institute, University of Limerick, Limerick, Ireland. Contact e-mails: James.Butler@staffmail.ul.ie and tofail.syed@ul.ie.

charge is directly discharged into the gaps between powders creating a high-energy heat source for sintering. The surface of the powder is activated because the oxidation film on the powder is broken down. Compared to the melting processes, samples can be fabricated in a short period of time at low temperatures and it is possible to produce high-purity samples. The advantages of SPS make it useful for the fabrication of intermetallic compounds for a variety of practical applications.

In contrast to previous studies on SPS of NiTi, our research aimed at the production of NiTi with density close to those produced by conventional vacuum melting methods. We also carried out mechanical working of the sintered material until a fine wire was obtained to allow, for example, tensile testing.

2. Experimental Details

Commercially pure powders of Ni (99.9 at.% purity) with an average particle size of about 5 μm and Ti (99.9 at.% purity) with an average particle size of about 30 μm were purchased from American Elements, USA (Fig. 1a and b). Ball milling is used to first obtain a homogeneous equiatomic NiTi powder mixture by quickly mixing the powders for 20 min in the presence of silicone nitride balls to enhance the mixing effect. The powders were shipped and stored under Argon gas. They were weighed and ball milled in air in a sealed container. The aspired NiTi 50:50 ratio was chosen with the aim to have the final wire's A_f below body temperature taking into consideration the intermetallics that form during this process. This is followed by cold compaction directly after the ball milling and SPS sintering immediately after that.

High grade graphite was used for making the SPS die and sintering was performed in vacuum ($\sim 10^{-3}$ Torr). SPS was carried out using a Dr. Sinterlab SPS 515S apparatus (Sumitomo Coal Mining Co. Ltd., Japan). The powder sample was packed in a high strength and high grade, ∅ 10 mm graphite die, and placed in between an upper and lower graphite electrode of the same grade and quality as that of the die. In the SPS apparatus, a pulsed direct current is applied through the sample electrodes and through the sample. 12 current pulses and two off-current pulses were used, known as a 12/2 sequence. The sequence of 12 ON pulses followed by 2 OFF pulses for a total sequence period of 46.2 ms, calculates to a characteristic time of a single pulse of about 3.3 ms. A uniaxial pressure of 50 MPa was maintained for the entire run. Sintering was carried out at 850 °C for 1 min, at 850 °C for 10 min, and 900 °C for 10 min.

After sintering the first 0.5 mm of NiTi material was removed from the billet diameter (10 mm diameter billet reduced to 9 mm billet) to eliminate the risk of carbon contamination.

The differential scanning calorimetry (DSC) was carried on a Perkin Elmer Pyris 1 calorimeter connected to an intercooler. Experiments were carried out at a cooling/heating rate of 10 °C/min in the temperature range of −65 to 120 °C using Helium as the purge gas. Samples were cut from the billet and extrudates, 40-50 mg each, and placed in aluminum pans so that the samples made good contact with the pan and cover.

Extrusions were carried out on a purpose built lab scale extruder and the billets were canned in $Cu_{10}Ni$ copper alloy prior to all extrusions. The can was in turn sealed in the extrusion barrel with a glass film that provided lubrication as well as a sealing to stop oxidization. All extrusions were carried out at 875 °C. A 0.7 mm wire was produced after a 4:1 area reduction followed by two 6:1 area reductions. The can was removed by pickling in concentrated nitric acid followed by mechanical polishing after the third extrusion. A full description of our extrusion setup can be seen on an earlier paper (Ref 19).

Microstructural analyses was carried out using SEM/EDX measurements to determine phases present in as-sintered and as-extruded materials. Hardness measurements were carried out on a LECO micro-hardness tester using a Vickers indenter tip with a 1 kg (9.81 N) load, dwell time under load of 15 s.

Tensile tests were carried out on a Hounsfield tensile tester fitted with a clip on extensometer for the measurement of the upper and lower loading plateaus. All test samples were 150 mm in length and were clamped in wedge type grips with emery paper between the wires being tested and the grip faces. Tensile tests were carried out first at a strain rate of 0.1 mm/min to establish the loading and unloading plateaus of the wire. A preload of 5 N was used, strained in increments of 1% strain until 4% strain followed by unloading to 5 N after each increment. The wire was then tensile tested at a strain rate 0.5 mm/min to establish the ultimate tensile stress (UTS) and strain to failure.

Oxygen was measured as per "ASTM E1019-08/CTP 3097/IG" and carbon was measured as per "ASTM E1019-08/CO" in an independent laboratory accredited through Nadcap and the American Association of Laboratory Accreditation (A2LA).

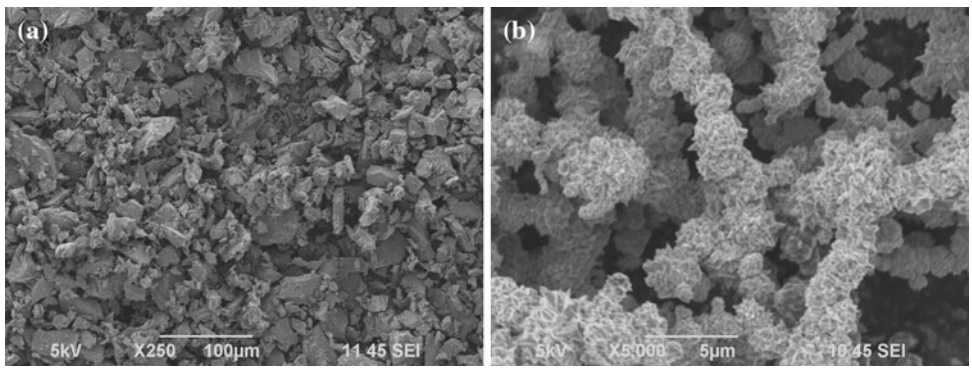

Fig. 1 Scanning electron micrograph of as-received elemental powders of (a) Ti and (b) Ni

3. Results and Discussion

The elemental powders of Ni and Ti were mixed equiatomically, but the as-received Ti powder had to be sieved to 20 μm to improve the final microstructure after sintering, Fig. 2(a). Table 1 shows the elemental analysis in atomic percentages as obtained from EDX on these microstructures.

The gas analysis was carried out according to ASTM E1019-08 and the results show that the carbon level in the SPS billet was 0.06 at.%, which is agreeable to the acceptable level set by the ASTM standard. The oxygen content measured 0.007 at.% is far less than that in commercially melted NiTi. Considering the purity of the starting powders (99.9 at.%) and the fact that mixing was done in a ball mill without any special precautions to stop oxidization, albeit in a short time of 20 min, this is a remarkably low level of oxygen, perhaps due to the nature of spark plasma sintering.

High amounts of NiTi phase with some nickel-rich and titanium-rich phases were found in all sintering conditions observed, e.g., Table 1. On the basis of EDX analysis, it can be concluded that the dark gray phase represent elemental Ti (Table 1(a), Spectrum 1 and 4) or a titanium-rich phase (Ti_2Ni) (Table 1(a), Spectrum 2). A nickel-rich phase (Ni_3Ti) (Table 1(b), Spectrum 1) was also present where the Nickel powder agglomerated. This nickel-rich phase was found very infrequently in the sintered material and extruded wire. The bulk analysis (Table 1(b), Spectrum 3) shows a slightly nickel-rich bulk chemistry.

The sintering of powders in the SPS begins with necking between particles, followed by densification before closed porosity is reached and finally the isolated pores are closed. The densification mechanism depends on many factors, e.g., material, particle size and shape, pressure, temperature, and time. There are several mass transport mechanisms which take place including surface diffusion, volume diffusion, grain boundary diffusion, viscous flow, plastic flow, and vapor transport from solid surfaces. In SPS, the sintering is further aided by the application of uniaxial pressure which promotes plastic deformation, dislocation creep, and diffusional creep.

The real time SPS profile (Fig. 3) shows the variation of temperature, pressure, and displacement of a typical run as a function of time. The holding time used in a typical sintering was 10 min. This holding time resulted in a higher volume fraction of NiTi and smaller amounts of other phases, mainly Ti_2Ni and Ni_3Ti. Furthermore, interatomic diffusion of the constituent elements allowed the mixture to approach the stoichiometric composition and resulted in the reduction of the amount of Ni_3Ti phase. These extra phases do not seem to affect the bulk properties and align in the extrusion direction in a banded structure, see Fig. 2(b).

The sintering temperature and extrusion parameters were optimized by using density and hardness data combined with microstructural observations. This ensured that the best densified material is obtained with correct functional properties. The hardness of the billet, sintered at 900 °C for 10 min, was 410 HV and the value dropped to 310 HV after three extrusions, first a 4:1 area reduction to break the as-sintered structure followed by two 6:1 area reductions resulting in a 0.7 mm wire. If a

Table 1 EDX chemical analysis of various points (a) in Fig. 2(a) and (b) in Fig. 2(b)

	Ti, at.%	Ni, at.%
a		
Spectrum 1	96.38	3.62
Spectrum 2	70.25	29.75
Spectrum 3	52.73	47.27
Spectrum 4	90.62	9.38
Spectrum 5	52.89	47.11
b		
Spectrum 1	26.35	73.65
Spectrum 2	51.13	48.87
Spectrum 3	49.43	50.57

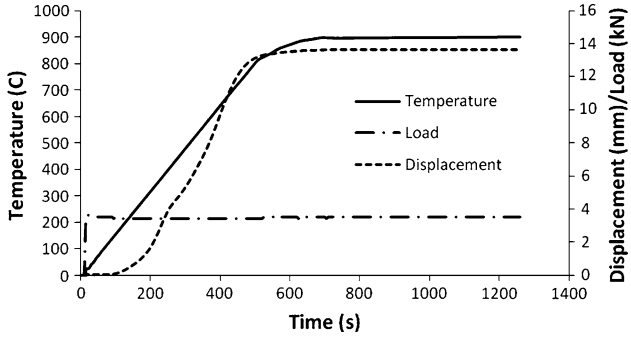

Fig. 3 Profile of the SPS data during a typical run, showing the temperature, load, and displacement plotted against time

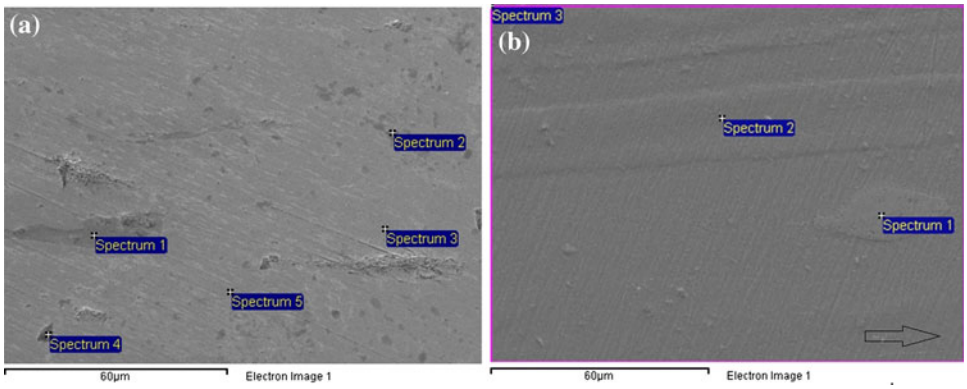

Fig. 2 SEM micrographs of samples (a) sintered at 850 °C for 1 min and (b) sintered at 900 °C for 10 min and then extruded three times (extrusion direction marked with an arrow). A banded structure orientated in the extrusion direction, right to left can be seen in (b)

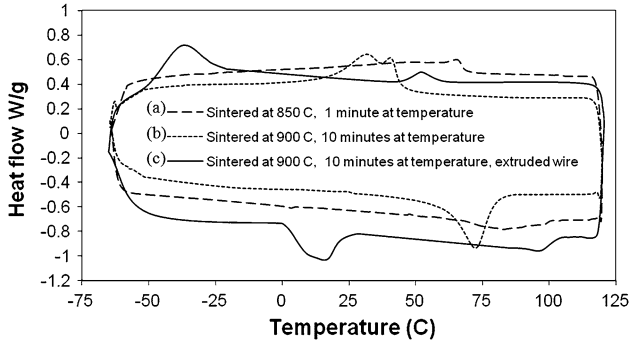

Fig. 4 The differential scanning calorimetry data showing endothermic and exothermic peaks for (a) a billet sintered at 850 °C for 1 min, (b) a billet sintered at 900 °C for 10 min, and (c) a wire produced from (b) followed by three extrusions and a heat treatment at 500 °C for 15 min

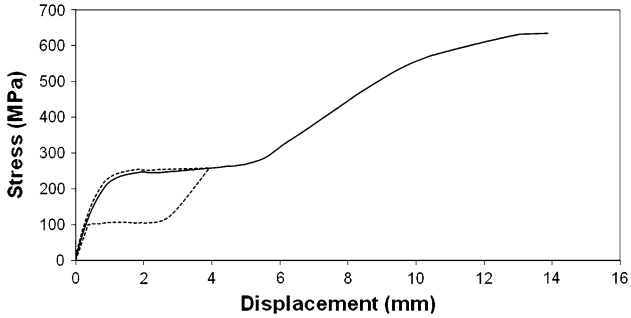

Fig. 5 Tensile test data of the 0.7 mm wire produced by sintering the elemental powders at 900 °C for 10 min, followed by three extrusions and a heat treatment at 500 °C for 15 min. A full tensile test for recoverable strain (dashed line) and to fracture (solid line) is shown

higher SPS temperature than 900 °C or pressure over 50 MPa was used, the metal would have flashed out at the punch. The density after sintering with these optimized settings was calculated to be 98.5% of the theoretical density taken as 6.5 g/cm^3. The microstructural analysis showed that the extrusion process decreased the residual porosity and the average pore dimension, as observed in SEM, was below l μm in size.

The initial cold compact of powder was 40 mm in height and there was almost 14 mm of compaction during the sintering process, with the final height of the sintered billet being 26 mm. It is interesting to see that the compaction during sintering started as low as 200 °C and stopped at about 850 °C, Fig. 3. The amount of time the sample is held at the optimal 900 °C sintering temperature is an important SPS parameter as shorter sintering times produced samples with far poorer tensile properties. Samples were also sintered at 850 °C for 10 min but these also had poor tensile properties. This indicated that even though the compaction would not proceed further at temperatures beyond 850 °C, pore fill up through interdiffusion, improved the density, compositional homogeneity and mechanical properties in billets sintered at 900 °C for 10 min.

A reaction between the graphite die and the NiTi powder during sintering is unavoidable with the standard SPS setup and may well affect the alloy composition. With the removal of 0.5 mm of NiTi material from the sintered billet diameter, the risk of this contamination affecting the properties of the bulk material was eliminated. The carbon pickup from the graphite die can be eliminated by using the Ti-cladding technique similar to the one used in (Ref 20), but these experiments have shown that this is not necessary as the low-carbon content achieved, with the standard setup used in these experiments, produces NiTi on par with the ASTM specifications.

The DSC results in Fig. 4, not only show the transformation temperatures but also the effect of processing history of the transformation temperatures. Both the as-sintered and extruded NiTi, using the optimal sintering parameters identified above, showed well-defined transformation peaks on cooling and heating, similar to those of melt-cast NiTi alloys. On the other hand, the transformation temperatures of the billet sintered at 850 °C prior to extrusion, showed weak endothermic and exothermic peaks (Fig. 4) and following extrusion. The wire produced from the billet sintered at 900 °C after three extrusions, received a heat treatment at 500 °C for 15 min, followed by water quenching. This improved the transformation properties further as would be expected.

Figure 4 then highlights the importance of the sintering parameters, e.g., temperature and holding time at temperature, in obtaining the shape memory effect. The extrusion process further promoted interdiffusion of the remaining non-NiTi phases resulting in only a small amount of titanium-rich phase affecting the transformation as indicated by the peak at 90 °C on heating and 55 °C on cooling. The A_f temperature of the NiTi wire in Fig. 4, was 20 °C by the tangent method on the peak between 0 and 25 °C on the heating part of the curve. This Ti-rich phase does not seem to have a large effect on the bulk properties of the extruded wire as described below in the tensile testing discussion.

The permanent set during tensile testing was measured to be ~0.2% for a 2% strain and increased to ~0.5% for a 4% strain. The loading and unloading cycling was stopped after 4% strain was reached as the permanent set was becoming too large. The extruded wire had an upper loading plateau of 254 MPa measured at a 2% strain and a lower loading plateau of 105 MPa, Fig. 5. The upper loading plateau extends to 5% strain where plastic deformation occurs at 267 MPa. At the end of the plateau there is a slow increase in the stress up to the UTS of 631 MPa where it finally ruptures. The material shows high ductility with the rupture finally occurring at a strain of 14%. The wire measured 0.6 mm in the middle of the gage length after tensile testing to failure which equates to a 36% area reduction in the middle of the gage length before failure. This indicated the material is highly cold drawable. The tensile properties will further refine during cold drawing which is normal during NiTi manufacturing, but is not attempted here.

4. Conclusions

We have demonstrated that the SPS sintering method is very effective in lowering the amount of impurities and other secondary phases in as-sintered NiTi alloys. Dense intermetallic compounds of NiTi were fabricated by SPS from elemental Ni and Ti powders. The majority of the matrix was essentially stoichiometric NiTi. The remaining non-NiTi phases formed a banded structure after extrusion and did not seem to affect the mechanical properties of the extruded wire. The resulting wire showed chemical homogeneity, low porosity and large shape

memory and superelastic effects with recovery strains of over 4% for an applied stress of 250 MPa. As a result of these findings, the processes described in this article may provide an alternative cost effective route for NiTi production.

Acknowledgment

This study was supported by Enterprise Ireland Innovation Partnership (IP/2008/545).

References

1. L. Krone and E. Schüller, Mechanical Behaviour of NiTi Parts Prepared by Powder Metallurgical Methods, *Mater. Sci. Eng. A*, 2004, **378**, p 185–190
2. M. Bram and A.A. Khanlou, Powder Metallurgical Fabrication Processes for NiTi Shape Memory Alloy Parts, *Mater. Sci. Eng. A*, 2002, **337**, p 254–263
3. E. Schüller and M. Bram, Phase Transformation Temperatures for NiTi Alloys Prepared by Powder Metallurgical Processes, *Mater. Sci. Eng. A*, 2004, **378**, p 165–169
4. J. Mentz and J. Frenzel, Powder Metallurgical Processing of NiTi Shape Memory Alloys With Elevated Transformation Temperatures, *Mater. Sci. Eng. A*, 2008, **491**, p 270–278
5. M. Köhl and T. Habijan, Powder Metallurgical Near-Net-Shape Fabrication of Porous NiTi Shape Memory Alloys for Use as Long-Term Implants by the Combination of the Metal Injection Molding Process with the Space-Holder Technique, *Adv. Eng. Mater.*, 2009, **11**(12), p 959–968
6. F. Neves, I. Martins et al., Reactive Extrusion Synthesis of Mechanically Activated Ti-50Ni Powders, *J. Intermet.*, 2007, **15**, p 1623–1631
7. F. Neves, I. Martins et al., Mechanically Activated Reactive Forging Synthesis (MARFOS) of NiTi, *J. Intermet.*, 2008, **16**, p 889–895
8. J. Mentz, M. Bram, et al., Improvement of Mechanical Properties of Powder Metallurgical NiTi by Reduction of Impurity Phases, *Proceedings of the International Conference on Shape Memory and Superelastic Technology 2006*, 2006, p 399–408
9. B. Bertheville and J.E. Bidaux, Alternative Powder Metallurgical Processing of Ti-Rich NiTi Shape-Memory Alloys, *Scr. Mater.*, 2005, **52**, p 507–512
10. S.K. Sadrnezhaad and A.R. Selahi, Effect of Mechanical Alloying and Sintering on Ni-Ti Powders, *Mater. Manuf. Process.*, 2004, **19**(3), p 475–486
11. M.D. McNeese, D.C. Lagoudas et al., Processing of TiNi From Elemental Powders by Hot Isostatic Pressing, *Mater. Sci. Eng. A*, 2000, **280**, p 334–348
12. C. Shearwood and Y.Q. Fu, Spark Plasma Sintering of TiNi Nano-Powder, *Scr. Mater.*, 2005, **52**, p 455–460
13. Y.Q. Fu and Y.W. Gu, Spark Plasma Sintering of TiNi Nano-Powders for Biological Application, *Nanotechnology*, 2006, **17**, p 5293–5298
14. A. Pozdnyakova, A. Giuliani et al., Analysis of Porosity in NiTi SMA's Changed by Secondary Pulse Electric Current Treatment by Means of Ultra Small Angle Scattering and Micro-Computed Tomography, *Intermetallics*, 2010, **18**, p 907–912
15. J. Frenzel, E.P. George et al., Influence of Ni on Martensitic Phase Transformations in NiTi Shape Memory Alloys, *Acta Mater.*, 2010, **58**(9), p 3444–3458
16. J.C. Hey and A.P. Jardine, Shape Memory TiNi Synthesis from Elemental Powders, *Mater. Sci. Eng. A*, 1994, **188**, p 291–300
17. T. Duerig, 1994, NiTi Alloys by Powder Metallurgical Methods, *The 1st Int'l Conference on Shape Memory and Superelastic Technologies*, p 31–42
18. M. Omori, Sintering, Consolidation, Reaction and Crystal Growth by the Spark Plasma System (SPS), *Mater. Sci. Eng. A*, 2000, **287**, p 183
19. J. Butler, P. Tiernan, et al., Processing of Small Scale Nitinol Billets by Induction Heated Non-Conventional Isothermal Extrusion (IHNCIE), *J. Eng. Mater. Technol.*, 2011, **133**(2)
20. J. Frenzel, Z. Zhang et al., High Quality Vacuum Induction Melting of Small Quantities of NiTi Shape Memory Alloys in Graphite Crucibles, *J. Alloys Compd.*, 2004, **385**, p 214–223